Analysis of Crack Severity on Power Density Increment of Gears

R. Saravanan[1, 2], Raghu V. Prakash[2], R. Gnanamoorthy[3], and Vinodkumar Boniface[1]
[1] Bangalore Engineering Centre, JFWTC, General Electric ITC, Bangalore, India
Email: Saravanan.r@geind.ge.com
Email: vinodkumar.boniface@ge.com
[2] Indian Institute of Technology, Madras/Department of Mechanical Engineering, Chennai, India
Email: raghuprakash@iitm.ac.in
[3] Indian Institute of Information Technology, Design and Manufacturing, (IIITD&M) Kancheepuram, /IIT Madras campus, Chennai, India
Email: gmoorthy@iitm.ac.in

***Abstract*— Helical gears are commonly used in industry as they have advantages of higher power density, quieter operation etc., compared to spur gears. Conventional gear design is based on various design criteria, including durability and bending strength load rating. In recent times, fracture failure modes are gaining importance in addition to conventional failure modes. Stresses due to operating fatigue loads and internal residual stresses can cause fatigue fracture failure on the surface, sub-surface of gear flanks or at tooth root of gears. During gear design, various parameters are optimized, and one such parameter is the helix angle that is optimized for power density and gear noise. However, effect of possible defects (voids and inclusions) in the gear tooth is not usually considered in these calculations. This paper is a study on severity of defects in a gear blank relative to power density increment. Three different gear geometries (spur and helical gears with two different helix angles) each with similar defects are considered. Finite Element Analysis (FEA) is used to analyze Tooth Interior Fracture (TIF), and study variation of Stress Intensity Factor (SIF) with crack size and helix angle. It is seen that power density increment of a common gear blank through helix angle increment poses a higher risk of crack severity, as the same gear blank is exposed to higher operating loads.**

***Index Terms*—gear, tooth interior fracture, linear elastic fracture mechanics, finite element analysis, power density, helix angle, voids, inclusions.**

I. INTRODUCTION

Cylindrical helical gears find wide application in modern power transmissions as they offer higher power density with increased contact ratio and quieter operation, when compared with spur gears. Durability (pitting) and bending strength load rating of gears may be calculated by methods detailed in ISO 6336-2&3 [1]. Durability (pitting) load rating is based on allowable contact stress, which is based on Hertzian contact theory. Bending strength load rating is based on allowable alternating tooth-root bending stress according to Lewis parabolic theory, as discussed in Dudley [2]. As material quality is a major parameter that directly impacts gear load ratings and is directly tied to material cleanliness, ISO 6336 [3] specifies cleanliness required for a gear material and defines the permissible size and quantity of voids and impurities. Gear blank forming processes such as rolling and forging tend to move and flatten inclusions and voids. The greater the defect size, the greater the grain structure disruption/discontinuity and the more likely it is to become a crack initiation point, and hence cause a negative impact on strength of the material. As discussed by Mack Aldener and Olsson [4], case-hardened gears are exposed to Tooth Interior Fatigue Fracture (TIFF) due to fatigue nature of operating and internal residual stress. In the present study, however, gears with different helix angles are studied for Tooth Interior Fracture (TIF) using 3D computational models based on fracture mechanics. This paper reports the various modes of fracture (Mode-I, Mode-II and Mode-III) in gears with varying power density.

II. GEAR TOOTH FINITE ELEMENT MODELING AND FRACTURE ASSESSMENT

This paper deals with the Tooth Interior Fracture (TIF) in a gear, which is different from Tooth Interior Fatigue Fracture (TIFF). Here, crack propagation is not studied, but rather the propensity for an existing crack to result in catastrophic failure. Also, effect of internal residual stresses is not considered. These cracks are due to defects (voids/ inclusions) that may be present in a gear blank. Three different gear sets (spur, helix with angle of 7^o and helix with angle of 15^o) are considered. These gear sets have the same gear ratio, module, material and face-width, but have different tooth geometries due to helix angle changes. Similar cracks (size and location) are assumed in these gears. For FEA, only one gear tooth with one crack is modeled for each configuration, and the resulting crack edge stresses are analyzed for likelihood of fracture. FEA of this 3D fracture mechanics problem is done using ANSYS and 3DFAS [5] (3-Dimensional Fracture Analysis System). Linear Elastic Fracture Mechanics (LEFM) theory is used to analyze 3D elliptical cracks in isotropic materials as reported by Ozkan et. al, [6], and Stress Intensity Factors (SIFs) for all fracture modes are calculated.

A. Gear Design and Parameters

Common dimensions of the three gear sets mentioned earlier are given in Table-I. Material of these gear sets is assumed to be 18CrNiMo7-6. In these gear sets, pinions are the focus of this paper. Pinion geometry, power density (kW/ kg) and increments are given in Table-II.

DOI: 01.IJMMS.01.01.57

TABLE I
COMMON PROPERTIES OF GEAR SETS

Module	12.00	mm
Face width	324.00	mm
Z1	22.00	
Z2	45.00	
Gear ratio	2.05	
Centre distance	411.00	mm

TABLE II
GEOMETRIES OF PINION SETS

Gear	Spur gear	7 deg. Helical Gear	15 deg. Helical gear
Pitch diameter mm	264.00	266.10	273.31
Tip diameter mm	294.40	296.50	303.72
Power transmitted kW	463.15	463.15	463.15
Weight kg	128.19	130.67	139.32
Power density kW/kg	3.61	3.54	3.32
Power density Increment	102%	100%	94%
Contact Pressure over gear flank N/m^2	1.153E+09	1.152E+09	1.114E+09

B. Gear tooth FE Model, Loads & Boundary Conditions

Most of the earlier studies on gear fracture have focused on loading the gear flank with contact area aligned parallel to the gear-axis, which is a valid assumption for spur gears. For helical gears, however, the trace orientation depends on helix angle as shown in the Fig. 1. Since the aim of this investigation is to assess crack severity, a critical loading zone has to be decided that is common for both spur and helical gears. A 3D Finite Element (FE) model of a single gear tooth with unmodified tooth profile was modeled in ANSYS using 20-node tetrahedron elements, as shown in Fig. 2. The tooth model had approximately 5 million elements, and was constrained at the root in all Degrees Of Freedom (DOF). As shown in Fig. 2, the unit normal load along the contact trace is calculated and applied over the contact area as pressure. Transmittable power of the helical gear with 7° helix angle (i.e., 463.15kW) is chosen as the reference, and all three gear sets are assumed to transmit this power, though their actual power ratings may differ. Contact stresses for all cases are calculated using a commercial gear design package, according to Hertzian contact theory.

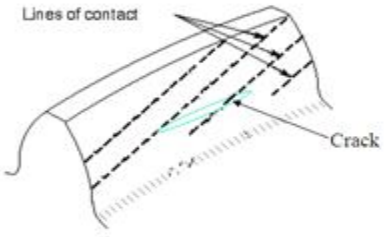

Figure 1. Cracked tooth model shows position of crack and load trace in helical gears

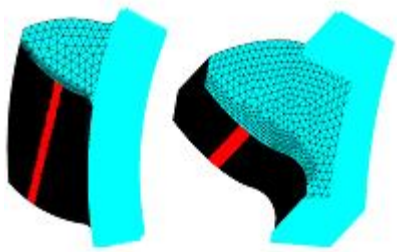

Figure 2. Contact load application over flank for Helical and Spur gears

As shown in Fig. 3 and Fig. 4, the single-mesh region of a gear pair in contact is highly loaded during power transmission, as only one pair of meshing teeth carries the entire transmitted load. In the double-mesh region, however, more than one pair share the transmitted load. Hence, the single-mesh region is critical loading region, and crack severity in a gear tooth in this region will be addressed.

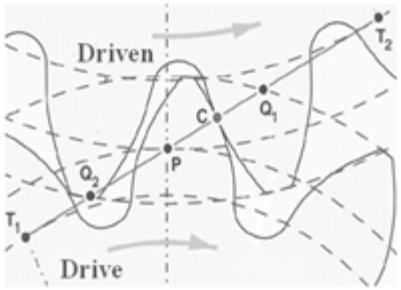

Figure 3. Gear mesh path

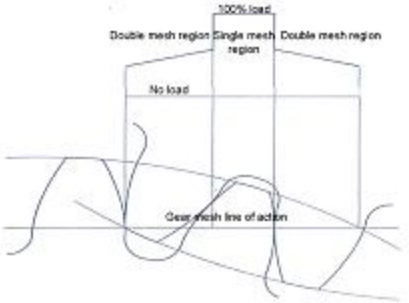

Figure 4. Gear mesh shows the critical loading zone

The normal pressure *p(x)* is a function of the maximum contact pressure, which is given by

$$p(x) = p_0 \sqrt{1 - \frac{x^2}{C^2}}$$

where

$$C^2 = \frac{4P}{HL}\frac{1}{\pi}$$

$$p_0^2 = \frac{PH}{L}\frac{1}{\pi}$$

$$H = \frac{\frac{1}{\rho_1} + \frac{1}{\rho_2}}{\frac{1-\mu_1^2}{E_1} + \frac{1-\mu_2^2}{E_2}} \qquad (1)$$

DOI: 01.IJMMS.01.01.57

Here, p_o is maximum contact pressure (MPa), F is normal force (N), C is half contact width (mm), E is modulus of elasticity (MPa), ρ is radius of curvature of gear tooth (mm), μ is Poisson's ratio, and L is effective face width (mm).
This pressure is applied in the single-mesh zone of all gear models as shown Fig. 5 and Fig. 6 to find SIFs for all fracture modes due to these contact loads.

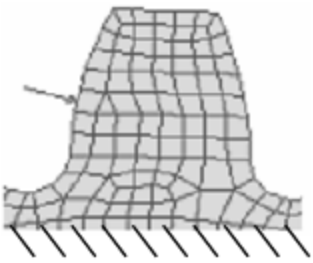

Figure 5. Load application in single mesh zone

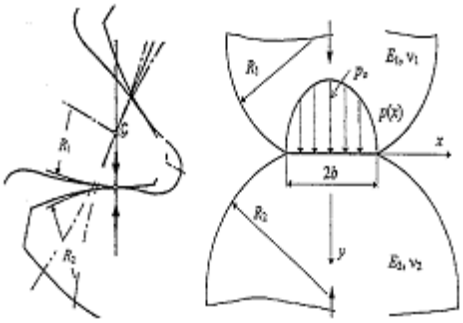

Figure 6. Load application over the contact area of the pinion as pressure.

C. Crack modeling and Fracture mechanics approach

It is assumed that all pinions are machined from blanks with similar defects – i.e., defects have the same size, shape and location. Defects are modeled as 3D elliptical cracks with finite dimensions. Crack centers are located below the mid-flank of the tooth at 7.5mm from loaded flank surface and 175mm from the gear tooth end. Seven different crack sizes (i.e. a= 0.1, 0.25, 0.5, 1.0, 2.0, 3.5, and 5.0 mm) with aspect ratio (= c/a) of 5 are modeled in each pinion model. Cracks (minor axis oriented in tooth thickness direction and major axis oriented along the tooth length) are inserted as shown in Fig. 7 using 3DFAS, where the quarter-point technique is used to simulate stress singularity according to LEFM. Here, the crack edge is surrounded by tunnel elements as shown in Fig. 8. A similar approach for crack edge refinement approach is found in Guagliano et al. [7]. Fracture properties for the pinion material are available in [8]. Critical SIF K_c=20MPa-m$^{1/2}$. Threshold values for crack growth are $?K_{I\_th}$~=3 to 7.5MPa-m$^{1/2}$ and $?K_{II\_th}$~= 1.5MPa-m$^{1/2}$.

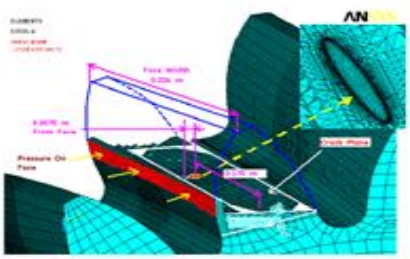

Figure 7. Cracked tooth models shows position of crack

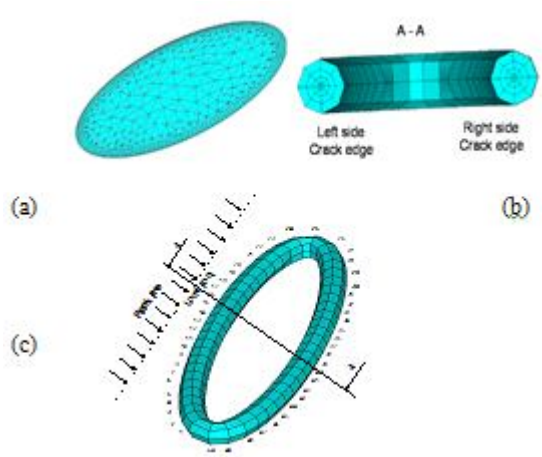

Figure 1. 3DFAS FE Model (a) Elliptical Crack plane close-up view of the mesh (b) Close-up view of tunnel mesh, (c) Elliptical crack edge surrounded by Tunnel element.

As reported in literature [9], grain size has an effect on the Tooth Interior Fracture for cracks below 10 times the grain size. Grain size of through-hardened forged and rolled steel is 5mm as per ISO 6336-5 [3]. Here, the initial crack length is larger than 0.05mm (10 times the grain size) and so LEFM is used. As this study deals with 3D spur and helical gear models, it is useful to evaluate fracture based on a combined SIF from all three fracture modes. The effective SIF for plane strain is computed as (Fajdiga et al. [10])

$$K_{eff} = \sqrt{\left(K_I^2 + K_{II}^2\right) + \left(1+\upsilon\right)K_{III}^2} \qquad (2)$$

where ν is the Poisson's Ratio. SIF values for all fracture modes around the 3D elliptical crack edges are obtained using local coordinate system.

III. RESULTS AND DISCUSSION

A. Effective Stress Intensity Factor (K_{eff})

All 3D gear tooth FE models (3 gear sets, with various crack sizes) are analyzed and SIFs around crack edges are obtained for the three fracture modes, viz., mode-I, II and III. It is possible to study the combined effect of these fracture modes, which presents a clear picture of fracture threshold for each gear models. As the models are loaded with pressure on selected nodes along the contact trace, there is a possibility of varying node density along this contact strip for different models. Effect of this variation can be reduced through use of effective SIFs (K_{eff}) that are shown in Fig. 9. From the K_{eff} plots, it is seen that these 3D elliptical cracks experience high SIF peaks at two locations – one close to the tooth surface and the other farther from it.

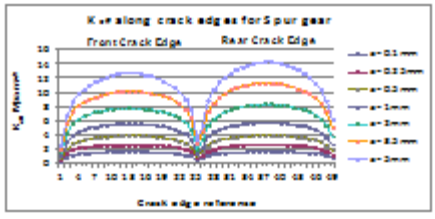

DOI: 01.IJMMS.01.01.57

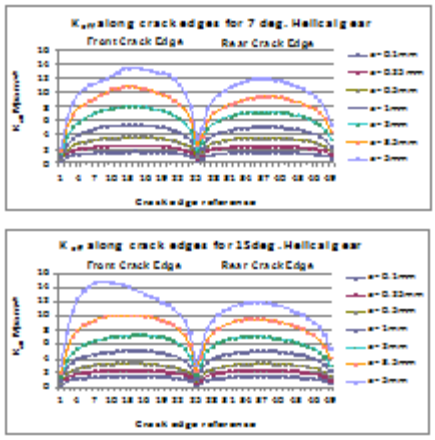

Figure 9. K_{eff} plots for all Pinions

B. *Crack sensitivity of all gears at crack edges*

To understand crack severity of all gear models, maximum K_{eff} values at crack edges are plotted against crack sizes as in Fig. 10. From these plots, it is seen that at small crack sizes, effect of helix angle is not seen. As crack size increases, the plots for the three gear sets tend to show differing trends. For the rear crack edge, this difference is more pronounced than the front crack edge. As mentioned earlier, a constant reference transmittable power (corresponding to the 7° helix angle) is used in the analysis of all three gear sets. If the actual transmittable power is used, it is likely that the 15° helical gear has higher K_{eff} values than 7° helical gear, and hence exhibits higher crack severity. Also, for large crack lengths, the front crack edge for the 15° helical gear interacts strongly with root, while the rear crack edge does not. However, the spur gear crack does not interact with the root on both edges. This is shown in Fig. 11.

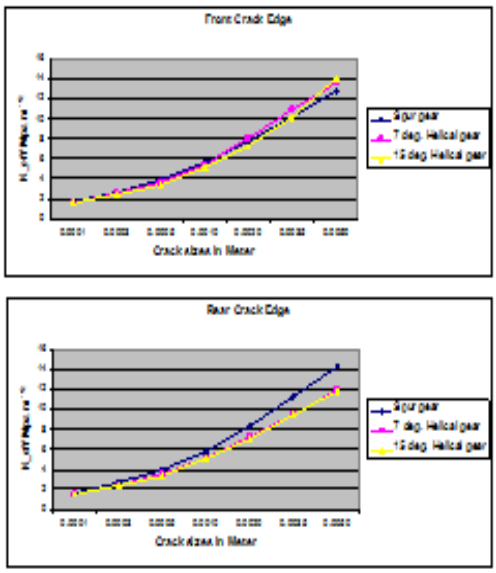

Figure 10. Trend of maximum K_{eff}

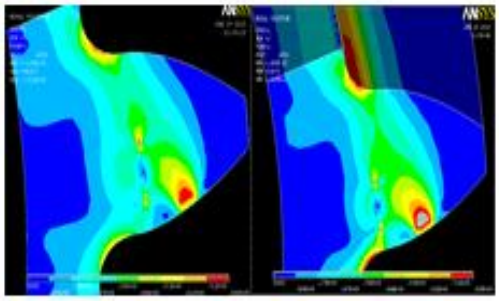

Figure 11. Von Mises stress plot for Spur and Helical gears for a=0.005mm

CONCLUSIONS

Form the study and analysis, it is seen that for helical gears, crack severity is higher for higher helix angles. Hence, care must be taken to assess crack severity over gear performance and ensure margin of gear strength through adequate reduction factors.

APPENDIX A NOMENCLATURE

a	crack length, mm
C	half contact width, mm
E	Modulus of elasticity, MPa
F	Normal force, N
K_{th}	threshold stress intensity factor, MPa $m^{1/2}$
K_c	critical stress intensity factor, MPa $m^{1/2}$
K_{eff}	effective stress intensity factor, MPa $m^{1/2}$
P_o	contact pressure, MPa
W	width of specimen, mm
Z1, Z2	number of teeth in pinion and gear respectively
□	Poisson's ratio
□	Radius of curvature of gear tooth, mm

REFERENCES

[1] ISO 6336-2&3:1996 Calculation of load capacity of spur and helical gears. Part 2: Calculation of surface durability (Pitting), Part 3: Calculation of tooth bending strength.
[2] Darle W. Dudley, Hand Book of Practical Gear Design, 1994.
[3] ISO 6336-5:2003 Calculation of load capacity of spur and helical gears Part 5: Strength and quality of materials.
[4] M. MackAldener and M. Olsson (2002): Analysis of crack propagation during Tooth Interior Fatigue Fracture. Engineering Fracture Mechanics, 69, 2147–2162
[5] 3DFAS Tutorial, GE GRC
[6] U. Ozkan, A.C. Kaya, A. Loghin, A.O. Ayhan, H.F. Nied (2006) Fracture Analysis of Cracks in Anisotropic materials using 3DFAS and ANSYS – 2006 ASME International Mechanical Engineering Congress and exposition – IMECE2006-15539
[7] M. Guagliano, L. Vergani and M.Virmercati (2007) Sub-surface crack propagation analysis in hypoid gears – Engineering Fracture mechanics (Article in press: Guagliano M et al., Sub-surface crack propagation analysis in hypoid gears, Eng Fract Mech (2007), doi: 10.1016/j.engfracmech.2007.03.025)
[8] Yan Ding, Rhys Jones and Bruce Kuhnell (1995) Numerical analysis of subsurface crack failure beneath the pitch line of a gear tooth during engagement – Wear, 185,141-149
[9] T.L Anderson, Fracture Mechanics – Fundamentals and application, 2nd edition. CRC press LLC, 1995.

DOI: 01.IJMMS.01.01.57

[10] G. Fajdiga, Z. Ren and J. Kramar (2007) Comparison of Virtual crack extension and strain energy density methods applied to contact surface crack growth. Engineering Fracture Mechanics (2007)

11] U. Ozkan, A.C. Kaya, A. Loghin, A.O. Ayhan, H.F. Nied (2006): Fracture Analysis of Cracks in Anisotropic materials using 3DFAS and ANSYS – 2006 ASME International [Mechanical Engineering Congress and exposition – IMECE2006-15539

DOI: 01.IJMMS.01.01.57